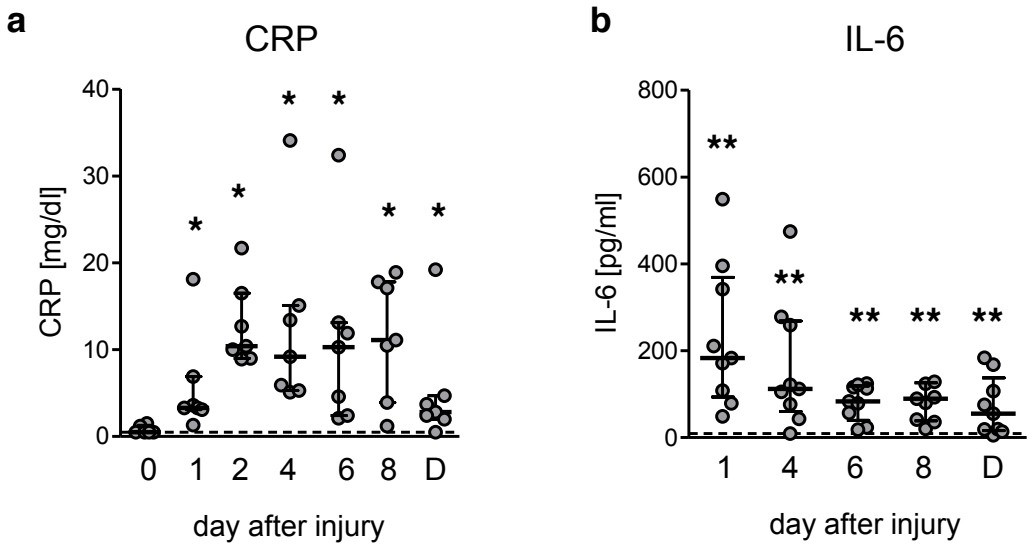

Supplementary Figure 1. Concentration of C-reactive protein and IL-6 in the serum after severe injury. **(a)** Kinetics of C-reactive protein (CRP) in the patients' sera from admission (day 0) to the day of discharge (D). **(b)** Concentration of IL-6 in the patients' sera (group 1). The broken lines indicate the standard value for healthy individuals (<0.5 mg/dl for CRP and <15 pg/ml for IL-6). Differences to the standard values were tested using the Wilcoxon Signed rank test. *, $p<0.05$; **, $p<0.01$ versus normal healthy control value

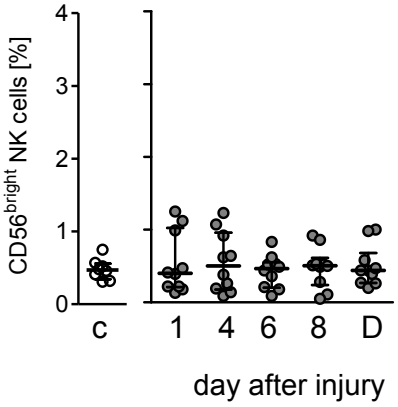

Supplementary Figure 2. Frequency of $CD56^{bright}$ NK cells. $CD56^{bright}$ NK cells from patients and healthy control subjects (group 1) were gated as shown in Fig. 1A. Data show individual values. Horizontal lines indicate the median and the interquartile range. No statistically significant differences were detected. c, control subjects; D, day of discharge

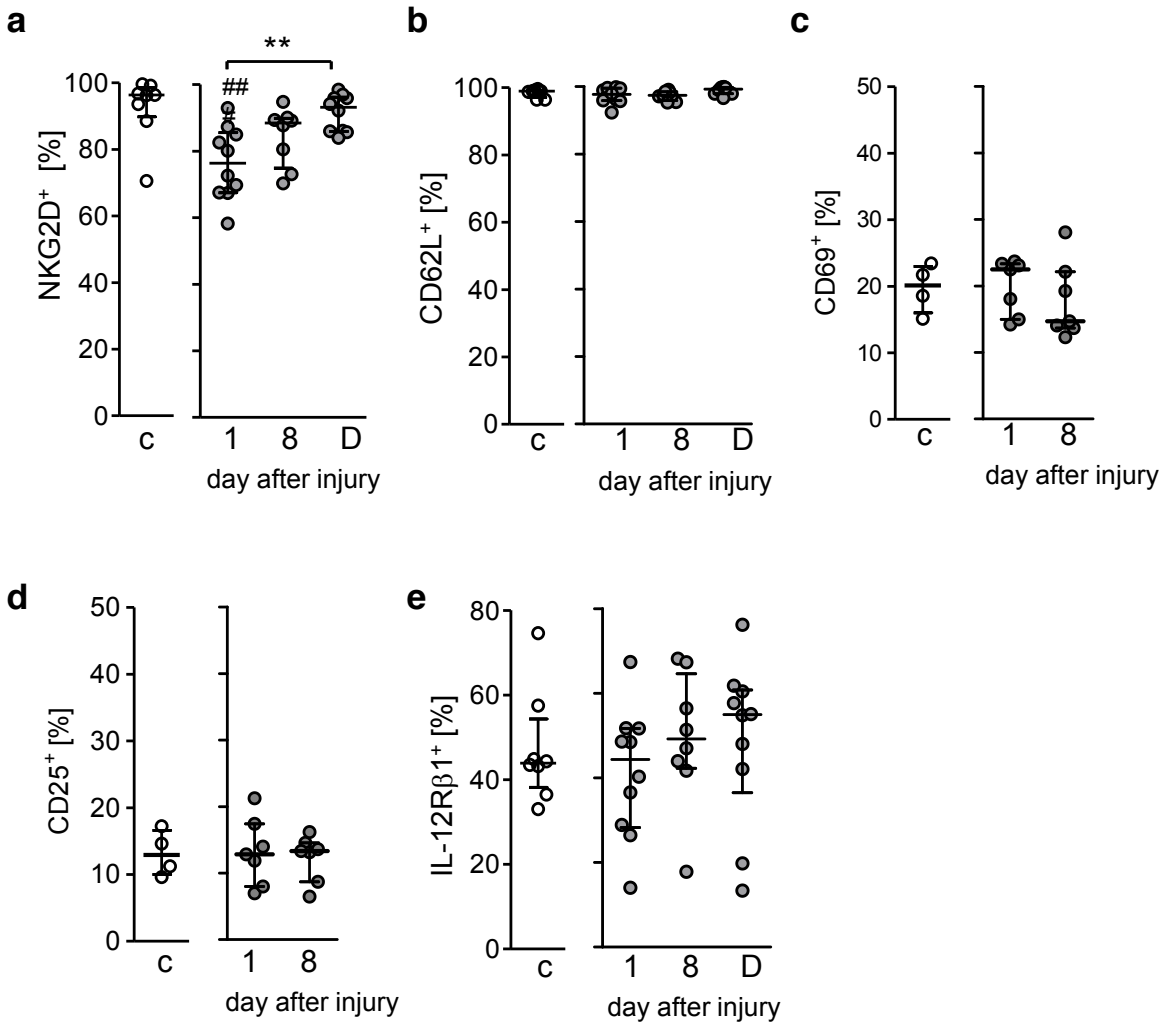

Supplementary Figure 3. Expression of diverse surface molecules on CD56^{bright} NK cells in systemic inflammation. PBMC from patients 1 and 8 d after severe injury and at the day of discharge as well as from healthy control subjects (group 1) were stained with antibodies against CD3 and CD56 in combination with antibodies against diverse surface molecules. The percentage of cells positive for NKG2D **(a)**, CD62L **(b)**, CD69 **(c)**, CD25 **(d),** and IL-12Rβ1 **(e)** among gated CD3^{-}CD56^{bright} NK cells was determined. The expression of CD69 and CD25 was examined on frozen/thawed PBMC. For gating see Fig. 1A. Data show the individual values. Horizontal lines indicate the median and the interquartile range. Differences between patients and control subjects were analyzed using the Mann Whitney U test. Differences between given time points after injury were examined using the Wilcoxon signed rank test. #, $p<0.05$; ##, $p<0.01$ versus controls. **, $p<0.01$. c, control subjects; D, day of discharge

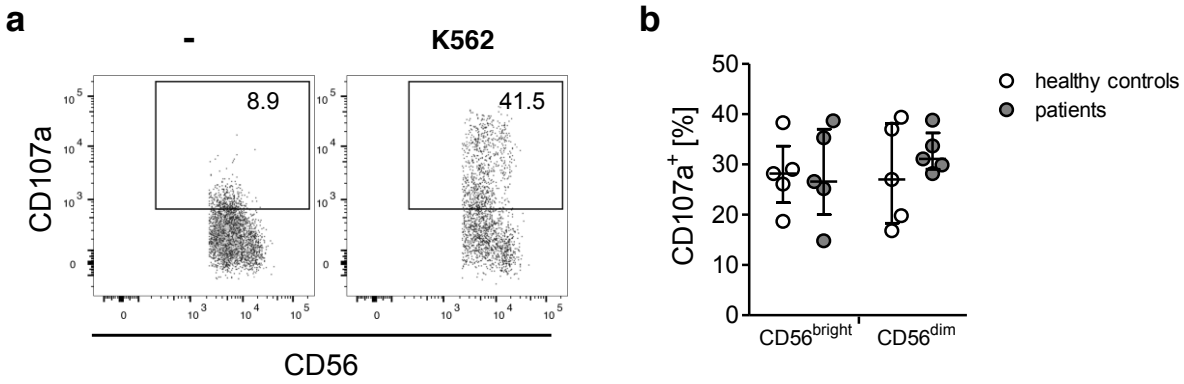

Supplementary Figure 4. Severe injury does not interfere with degranulation of NK cells. Frozen PBMC from healthy donors and from severely injured patients (d4 after injury) were used to determine target cell-induced degranulation. Degranulated NK cells were identified as $CD3^-CD56^+CD107a^+$ cells. (a) Dot plots of CD107a expression on gated $CD3^-CD56^{bright}$ or $CD3^-CD56^{dim}$ NK cells from one representative patient in the absence (-) or presence of K562 cells. Numbers indicate the percentage of $CD107a^+$ NK cells. (b) Specific degranulation was determined by substraction of spontaneous degranulation from values obtained in the presence of K562. Data show individual values of healthy control subjects and patients (each n=5). Horizontal lines indicate the median and interquartil range. No significant differences were observed.

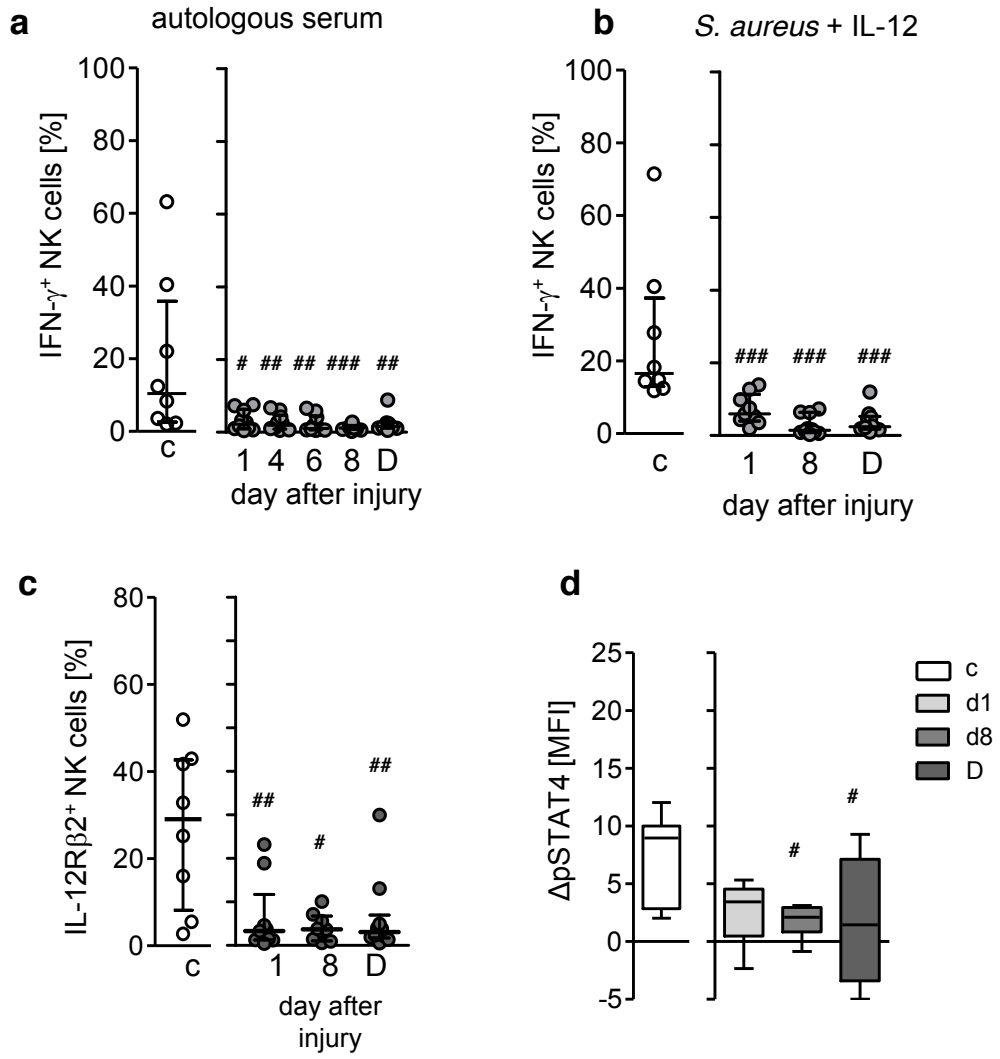

Supplementary Figure 5. Suppression of CD56^{dim} NK cells after injury. Cultures of PBMC from patients and control subjects (group 1) were set up in autologous serum and were stimulated with *S. aureus* in the absence (a, c, d) or presence (b) of recombinant IL-12 as described in Fig. 1c and Fig. 2b. The percentage of IFN-γ^+ cells **(a, b)**, IL-12R$\beta2^+$ cells **(c)**, and ΔpSTAT4 **(d)** was determined for gated CD3$^-$CD56^{dim} NK cells. Data show the individual values or Tukey box plots. Horizontal lines indicate the median and the interquartile range. Differences between patients and control subjects were analyzed using the Mann Whitney U test. #, $p<0.05$; ##, $p<0.01$; ###, $p<0.001$ versus controls. c, control subjects; D, day of discharge

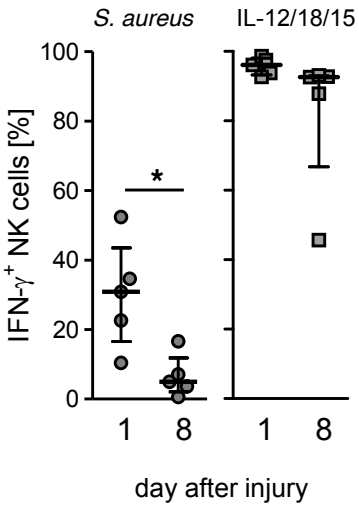

Supplementary Figure 6. Suppression of NK cells is overcome by exposure to strong cytokine-induced signals. Thawed PBMC from patients 1 d and 8 d after severe injury were set up in parallel and were stimulated with *S*. *aureus* or with a cocktail of IL-12, IL-18, and IL-15 in the presence of FCS. The IFN-γ synthesis in $CD56^{bright}$ NK cells was determined as described in Materials and Methods. Data show individual values (n=5). Horizontal lines indicate the median and interquartile range. Statistical analyses were performed using the Mann Whitney U test. *, $p<0.05$

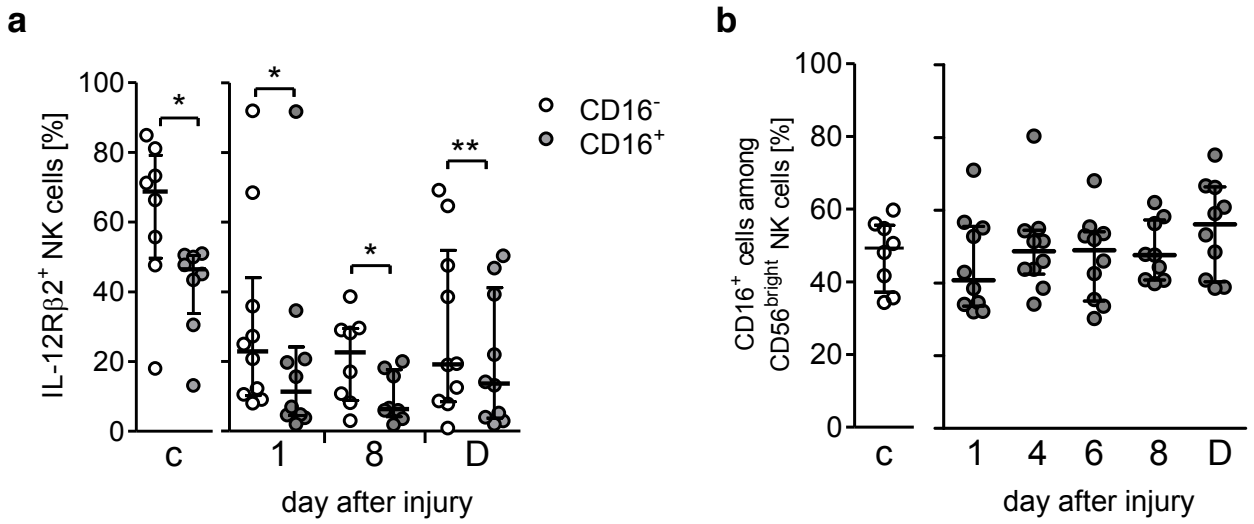

Supplementary Figure 7. Expression of IL-12Rβ2 on $CD16^{+}CD56^{bright}$ NK cells after injury. **(a)** Cultures of PBMC from patients and control subjects (group 1) were set up in autologous serum and were stimulated with *S. aureus* as described in Fig. 1C. The percentage of IL-12Rβ2^{+} cells in $CD16^{-}$ versus $CD16^{+}$ $CD56^{bright}$ NK cells was determined. Differences between $CD16^{-}$ and $CD16^{+}$ cells were analyzed using the Wilcoxon signed rank test. **(b)** Percentage of $CD16^{+}$ cells among gated $CD56^{bright}$ NK cells. No significant difference between cells of healthy controls and patients were detected. Data show the individual values. Horizontal lines indicate the median and the interquartile range.. *, $p<0.05$; **, $p<0.01$. c, control subjects; D, day of discharge

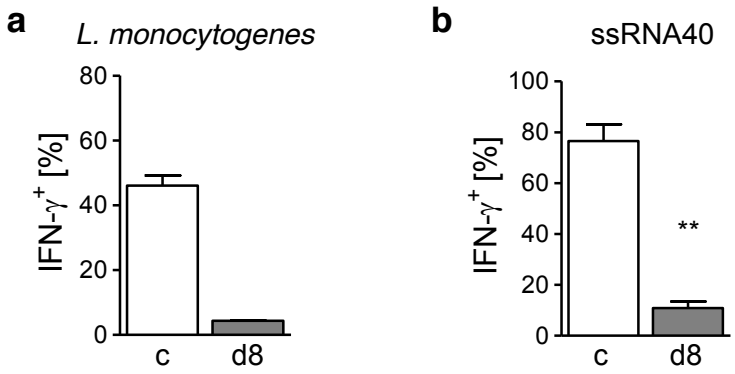

Supplementary Figure 8. The inhibitory activity of the patients' sera on $CD56^{bright}$ NK cells is not restricted to *S. aureus*-induced IFN-γ production. PBMC from healthy donors were stimulated with **(a)** inactivated *L. monocytogenes* or **(b)** ssRNA40 in the presence of 2 % pooled sera from patients 8 d after injury or from control subjects (group 1). The percentage of IFN-γ^+ cells among total $CD3^-CD56^{bright}$ cells was determined by flow cytometry as described in Fig. 1. Bar graphs show the mean+range of 2 donors (a) or mean+SEM of four donors (b). Statistical differences were tested using the paired Student's t-test. **, $p<0.01$. c, control subjects; D, day of discharge

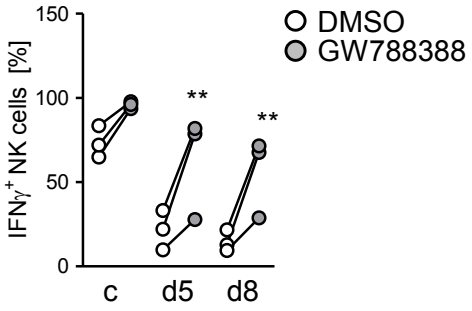

Supplementary Figure 9. The inhibitory activity of the patients' sera on CD56^{bright} NK cells is mediated by activin-like kinase 5. Cultures of PBMC from healthy donors were set up in pooled sera from control subjects (c) or from patients 5 and 8 days after injury. Cells were stimulated with inactivated *S. aureus* as described in the section Materials and Methods in the presence of the ALK5 inhibitor GW788388 or its solvent dimethyl sulfoxide (DMSO). The percentage of IFN-γ^+ cells among total CD3$^-$CD56^{bright} cells was determined as described in Fig. 1. Data from three individual experiments are shown. Statistical differences between DMSO and inhibitor were tested using the paired Student's t-test. **, $p<0.01$.

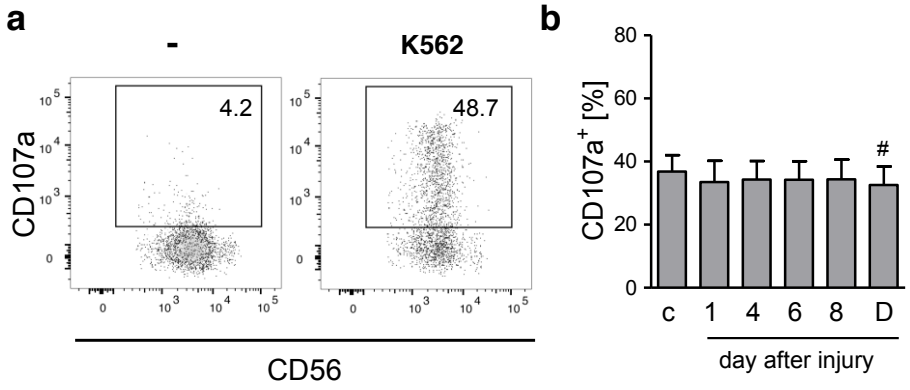

Supplementary Figure 10. Serum from patients does not affect the degranulation of NK cells. Cultures of PBMC from healthy donors were set up in medium containing 4 % pooled sera from patients at different time points after severe injury or of control subjects (group 1) and were incubated with or without K562 target cells. Degranulated NK cells were identified as $CD3^-CD56^+CD107a^+$ cells. **(a)** Dot plots of CD107a expression on gated $CD3^-CD56^+$ NK cells from one representative donor in the absence (-) or presence of K562 cells. Numbers indicate the percentage of $CD107a^+$ NK cells. **(b)** Specific degranulation was determined by substraction of spontaneous degranulation from values obtained in the presence of K562. Data are presented as mean+SEM of 5 experiments, each performed in duplicate. Significant differences between serum from controls versus serum from patients at different time points after injury were tested by Repeated Measures ANOVA followed by Dunnett's Multiple Comparison test. #, $p<0.05$ vs. control sera; c, healthy control sera; D, day of discharge

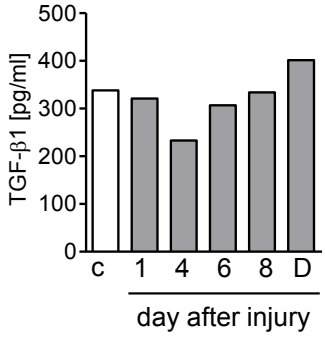

Supplementary Figure 11. Concentration of active TGF-β1 in the serum after severe injury. Sera from all patients (group 1) were pooled for each time point and the content of active TGF-β1 was determined by ELISA. Pooled serum from healthy donors was used as control. Data show the mean of triplicate values. C, control; D, discharge

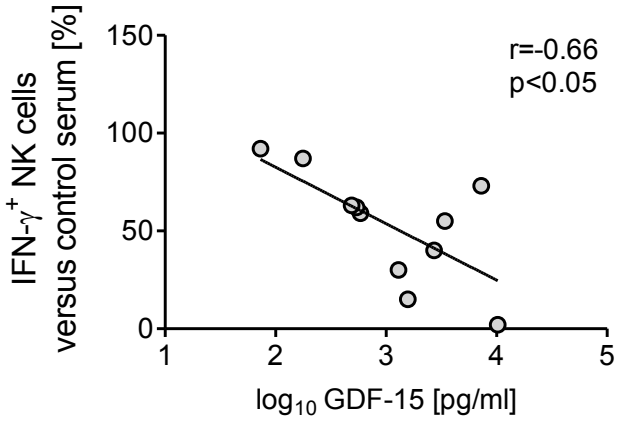

Supplementary Figure 12. Correlation of GDF-15 levels with the synthesis of IFN-γ in CD56^{bright} NK cells. Spearman correlation between the concentration of GDF-15 in the sera of individual patients (part of group 2; day 5 serum; n=11) and the synthesis of IFN-γ (normalized to pooled serum from healthy control subjects that was set as 100% as shown in Fig. 6d) on CD56^{bright} NK cells from healthy donors after exposure to the sera.

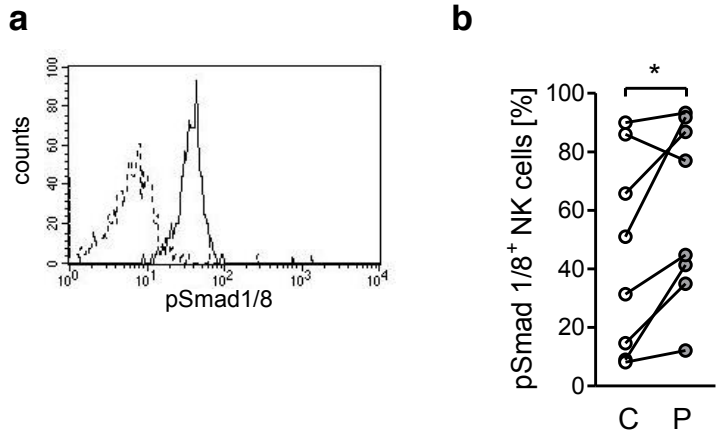

Supplementary Figure 13. Activation of Smad1/8 in CD56^{bright} NK cells after exposure to the patients' sera. PBMC from healthy donors were incubated in the presence of pooled sera from healthy control subjects (c) or from severely injured patiens on day 8 (P). Phosphorylated Smad1/8 (pSmad1/8) was determined in gated CD56^{bright} NK cells by intracellular flow cytometry. **(a)** Representative histogram of pSmad1/8 expression in CD56^{bright} NK cells in the presence of the patients' sera. The broken line indicates the isotype control staining. The threshold for positive staining was set at 1%. **(b)** Cumulative data of seven experiments. Statistical differences were tested using the Mann Whitney test. *, $p<0.05$

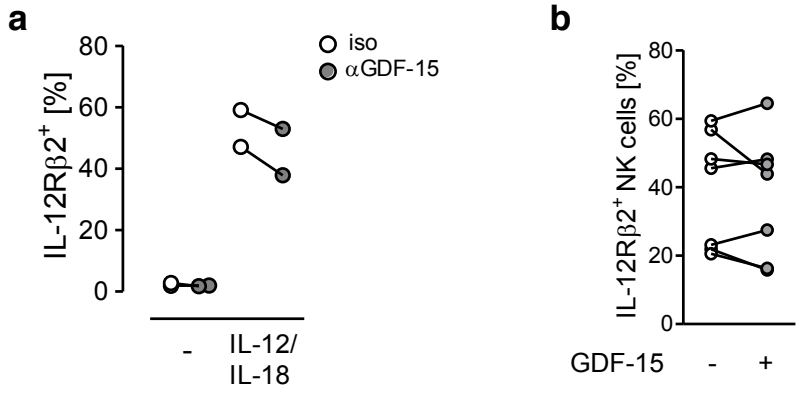

Supplementary Figure 14. Effect of GDF-15 on purified NK cells. **(a)** GDF-15 was removed from serum of healthy control subjects using specific antibodies (αGDF-15) as described in Materials and Methods. As control, the serum was treated with isotype control antibodies (iso). Purified NK cells from healthy donors (n=2) were cultured in the presence of the sera (at a final concentration of 2%) and were stimulated with IL-12/IL-18 for 18 h. **(b)** Purified NK cells from healthy donors (n=7) were cultured in the presence of 1% FCS and were stimulated with IL-12/IL-18 in the presence or absence of 10 ng/ml recombinant human GDF-15. The expression of IL-12Rβ2 on $CD56^{bright}$ NK cells was determined. No significant differences were detected. Data show the percentage of IL-12Rβ2$^+$ NK cells from individual donors.

Supplementary Figure 15. Putative Smad1/5 binding sites in the promoter of the *IL12RB2* gene. The sequence of the promoter (black) and its flanking regions (grey) of the human *IL12RB2* gene was obtained from ENSEMBL databank. The location of exon 1 is highlighted in brown. Putative bindings sites for Smad1/5 (core binding sequences: gGCGCc and gACGCc) were identified using the software GPMiner (http://gpminer.mbc.nctu.edu.tw/) and are labeled in red.